J. Math. Computer Sci., 40 (2026), 292–309

Online: ISSN 2008-949X

Journal of Mathematics and Computer Science

Journal Homepage: www.isr-publications.com/jmcs

Neural network framework for controllability of fractional Volterra Fredholm integro-differential equations with state-dependent delay

Prabakaran Raghavendran[a], Tharmalingam Gunasekar[a,b], Dumitru Baleanu[c,d], Shyam Sundar Santra[e,*], Debasish Majumder[e]

[a]*Department of Mathematics, Vel Tech Rangarajan Dr. Sagunthala R&D Institute of Science and Technology, Chennai-600062, Tamil Nadu, India.*

[b]*Department of Mathematics, Institute of Engineering and Technology, Srinivas University, Mukka, Mangaluru, Karnataka 574146, India.*

[c]*Department of Computer Science and Mathematics, Lebanese American University, Beirut 11022801, Lebanon.*

[d]*Institute of Space Sciences-Subsidiary of INFLR, Magurele-Bucharest, Romania.*

[e]*Department of Mathematics, JIS College of Engineering, Kalyani, West Bengal 741235, India.*

Abstract

This paper presents a new approach to analyzing the controllability of fractional Volterra-Fredholm integro-differential equations with state-dependent delay, characterized by the Caputo fractional derivative and governed by a semigroup of compact and analytic operators. Controllability results are derived using Schauder's fixed point theorem, addressing the challenges of fractional dynamics and state-dependent delays. A key innovation in this study is the integration of theoretical analysis with advanced computational methods, specifically Physics-Informed neural networks, to approximate solutions and verify controllability conditions. To validate the theoretical findings, a detailed example is provided, along with numerical simulations that confirm the convergence of solutions. Graphical representations offer additional insights into the solution dynamics, enhancing the understanding of the system's behavior. By combining mathematical rigor with machine learning techniques, this work establishes a computational framework for tackling complex fractional systems, paving the way for further exploration of their controllability.

Keywords: Controllability, Schauder fixed point theorem, physics-informed neural networks (PINNs), numerical simulations.

2020 MSC: 34A08, 45J05, 65L20, 93C23, 68T07.

1. Introduction

In recent years, the extensive applications of fractional Volterra-Fredholm integro-differential equations, particularly those with state-dependent delays, have garnered significant attention. These equations are characterized by the presence of fractional derivatives, allowing for the modeling of systems with

*Corresponding author

Email addresses: rockypraba55@gmail.com (Prabakaran Raghavendran), tguna84@gmail.com (Tharmalingam Gunasekar), dumitru.baleanu@lau.edu.lb (Dumitru Baleanu), shyam01.math@gmail.com or shyamsundar.santra@jiscollege.ac.in (Shyam Sundar Santra), debamath@rediffmail.com (Debasish Majumder)

doi: 10.22436/jmcs.040.03.01

Received: 2025-03-26 *Revised:* 2025-04-27 *Accepted:* 2025-05-12

memory effects and hereditary properties to be more accurate. One of the most fundamental resources for understanding fractional differential equations is the work of Zhou, which provides a comprehensive introduction to the basic theory of such equations, including key concepts and mathematical formulations [29]. More of this theoretical work together with applications regarding fractional differential equations is found in the comprehensive book by Kilbas, Srivastava, and Trujillo on the subject of fractional differential equations [19]. Fractional integro-differential equations with SDD are discussed here specifically by Agarwal and Andrade where the relevant issues characteristic for such systems have been discussed in the context of fractional integro-differential equations. The complexity of such modeling, since future behavior relies not only on the current state but also upon prior states is the main point of this paper [1]. Similarly, Benchohra and Berhoun, in their paper, extended the aforementioned result that impulsive fractional differential equations with SDD were investigated, providing an important contribution to the research on dynamic systems with sudden jumps and memory [3]. Guendouzi and Bousmaha, in their article, in highlighting the importance of the controllability of fractional systems, especially in systems with uncertainty and time-delays, found the approximate controllability of fractional neutral stochastic functional integro-differential inclusions with infinite delay [8]. Liu and Bin's contribution on impulsive Riemann-Liouville fractional differential inclusions gives a very important view of how the impulsive effects interact with fractional dynamics, complicating the solution methods [22].

Balasubramaniam and Tamilalagan's contribution towards the literature would be investigating approximation controllability using Mainardi's function-the important tool when it comes to the study delays and stochasticity in fractional systems [2]. A very influential work on fractional differential equations has appeared in the publication of Podlubny that extensively covers theory, as well as applications, concerning fractional calculus which makes this to be a valuable reference towards basic ideas applied within the study at hand [25]. The work of Mainardi et al. on probability distributions generated by fractional diffusion equations relates the connection between fractional derivatives and diffusion processes and sheds valuable light on the behavior of fractional systems [23]. In more recent studies, Gunasekar et al. investigate the existence and controllability of neutral fractional VFIDEs, shedding light on the complexities of these systems and presenting new results for their solution and control [10].

Hamoud's results on existence and uniqueness of the solution for fractional neutral VFIDEs are critical contributions to the theory of these systems, important to the well-posedness of these equations [13]. The paper by Hamoud et al. go beyond existence and uniqueness for VFIDEs and some significant theoretical inputs to this subject matter [15].

Contributing to this line of research is a work by Gunasekar et al. titled "application of Laplace transforms for solution of fractional integro-differential equations: the armory for solving these equations keeps on increasing" [9]. Recent work by Gunasekar and colleagues on the existence, uniqueness, and stability of neutral fractional VFIDEs provides significant results that form part of the theoretical framework required to understand the stability of these complex systems [11]. Columbu et al. work on chemotaxis systems introduces refined criteria for boundedness, which has relevance in the study of fractional systems with nonlinear dynamics [4]. New recent results by Hamoud and Ghadle on the uniqueness of solutions for fractional VFIDEs are going to bring in new insight to the structure and properties of such equations and to extend knowledge on the solution space of them [14]. Existence and uniqueness results on VFIDEs by using Caputo fractional derivative, due to Ndiaye and Mansal, bring about very crucial analysis to be used for this kind of equations [24]. Dahmani's work on the high-dimensional fractional differential systems introduces new results about existence and uniqueness, and more complex systems with fractional order can be better understood through this approach [6]. HamaRashid et al. introduce the topic for the existence of the Volterra-Fredholm integral equations of nonlinear boundary type and provide new numerical results that expand the understanding of boundary conditions in fractional systems [12]. Kalamani et al. contributions to impulsive fractional neutral stochastic integro-differential equations significantly aid the study of systems by simultaneously capturing the effects of impulsivity and stochasticity [18]. Lastly, Hernandez, Prokopczyk, and Ladeira contributions to partial functional differential equations with SDD bring in more theoretical frameworks in the study of systems with delay and

memory, giving deeper insights into the dynamics of such systems [16]. This paper intends to contribute to the increasing knowledge base on fractional VFIDEs, but especially for the purposes of controllability and SDDs. The research presented here develops from previous work foundations and provides a new approach for solving these systems, opening new avenues for further exploration.

Raghavendran et al. [26] deals with the existence, uniqueness, and stability of fractional neutral VFIDEs with SDDs. The paper brings to the reader a few significant mathematical results on the types of systems discussed above as well as an insight into the behavior of these systems under particular conditions of SDDs. These are critical to understand in systems governed by equivalent fractional equations when taken along with the control theory perspective. In this paper, we extend their findings by focusing on the controllability of systems described by such equations. More specifically, we investigate how SDDs affect the ability to reach desired states when applying certain control strategies, utilizing the mathematical framework developed by Raghavendran et al. [26] to derive conditions for the controllability of the fractional systems under study.

Recent explorations have deepened the intellection on chemotaxis phenomena and complexities modeled by fractional differential equations. Li et al. [21] modeled the combined effects of attraction and repulsion mechanisms with production and consumption dynamics, successfully giving boundedness criteria vital to stabilizing chemotaxis models. In studying parabolic chemotaxis systems, Jiao et al. [17] noted some challenges stemming from singular pattern functions and proliferation. Here, global existence of solutions has been guaranteed under some structural conditions. In the realm of integro-differential control theory, Prabakaran Raghavendran et al. [27] formulated a novel AI-based technique for examining the controllability of fractional impulsive neutral Volterra-Fredholm integro-differential systems with state-dependent delays, making valuable contributions to the effective management of systems exhibiting both memory and impulsive effects. Complementing this, Columbu et al. [5] focused on the long-term behavior of chemotaxis models and established uniform-in-time boundedness of solutions in a large class of local and nonlocal nonlinear attraction-repulsion models, even in the presence of logistic source terms. And in Li et al. [20], the authors further investigated how dissipative gradient nonlinearities avert δ-singularity formations, giving rigorous results on the applicability of nonlocal and local attraction-repulsion models and a better understanding of how nonlinearity prevents blow-up scenarios in chemotactic aggregations.

Ganesh et al. [7] investigate the Hyers-Ulam-Mittag-Leffler stability of fractional differential equations involving two Caputo derivatives by making use of the fractional Fourier transform as a salient tool for analysis. Being a generalization of the classical Fourier transform, this technique is instrumental in researching the robustness of behaviors of solutions of systems under fractional calculus-a field that is ever so growing in application to real-world complex phenomena. Related to this work, Santra et al. [28] look at oscillation criteria of first-order nonlinear neutral differential equations with multiple delays. Such results provide sufficient conditions for the oscillatory nature of these equations, thereby extending the knowledge of time-delay systems that occur frequently in engineering and biological models.

In this study, we investigate the controllablity results of mild solutions for a class of fractional VFIDEs with SDD, described by the following system:

$$\begin{aligned} {}^{c}D^{\rho}\eta(\aleph) &= \mathcal{A}\eta(\aleph) + g(\aleph, \eta_{\rho(\aleph,\eta_t)}) + \int_{\aleph_0}^{\aleph} Z_1(\aleph,\sigma,\eta_{\rho(\sigma,\eta_s)})d\sigma + \int_{\aleph_0}^{b} Z_2(\aleph,\sigma,\eta_{\rho(\sigma,\eta_s)})d\sigma + Bu(\aleph), \\ \aleph &\in J = [\aleph_0, b],\ 0 < \rho < 1, \quad \eta(\aleph_0) = \eta_0 = \varphi(\aleph) \in \mathcal{B}, \quad \aleph \in (-\infty, 0]. \end{aligned} \tag{1.1}$$

Consider $\eta(\cdot)$, an unknown function taking values in the Banach space X with norm $\|\cdot\|$. We focus on the Caputo fractional derivative ${}^{c}D^{\rho}$ of order $0 < \rho < 1$, where $\mathcal{A}$ represents the infinitesimal generator of a compact, analytic semigroup $\{T(\aleph), \aleph \geqslant 0\}$ of uniformly bounded linear operators in X. Functions $g : J \times \mathcal{B} \to X$ and $Z_i : D \times \mathcal{B} \to X$ for $i = 1, 2$ are suitably defined, with $D = \{(\aleph, \sigma) \in J \times J : \aleph_0 \leqslant \sigma \leqslant \aleph \leqslant b\}$. Additionally, $\rho : J \times \mathcal{B} \to (-\infty, b]$ is appropriately specified.

The initial condition $\varphi \in \mathcal{B}$ satisfies $\varphi(0) = 0$. Here, $\mathcal{B}$, defined in the preliminary section, serves as the phase space. For any continuous function η defined on $(-\infty, b]$ and $\aleph \geqslant 0$, η_t denotes the element

of $\mathcal{B}$ given by $\eta_t(\theta) = \eta(\aleph + \theta)$ for $\theta \leqslant 0$. This function $\eta_t(\cdot)$ encapsulates the state history from each $\theta \in (-\infty, 0]$ up to the current time $\aleph$. The control function $u(\cdot)$ resides in $L^2(J, U)$, a Banach space of admissible control functions, where U is a Banach space, and B represents a bounded linear operator from U into X.

2. Preliminaries

In this section, we focus on the commonly used definitions in fractional calculus, including the Riemann-Liouville fractional derivative and the Caputo derivative, as discussed in various academic studies [8, 11, 16]. The Banach space $C(J, X)$, where $J = [\aleph_0, b]$, is endowed with the supremum norm. For any $\eta \in C(J, X)$, this norm is expressed as $\|\eta\|_\infty = \sup\{|\eta(x)| : x \in J\}$.

Definition 2.1 ([11, 16])**.** Let $\rho > 0$ denote the order of integration, and let φ be a given function. The fractional integral of φ based on the Riemann-Liouville definition is expressed as

$$J^\rho \varphi(\tau) = \frac{1}{\Gamma(\rho)} \int_0^\tau (\tau - \aleph)^{\rho-1} \varphi(\aleph) d\aleph, \quad \text{for } \tau > 0 \text{ and } \rho \in \mathbb{R}^+,$$

where $\Gamma(\cdot)$ denotes the Gamma function, and $\mathbb{R}^+$ represents the set of positive real numbers. By convention, $J^0\varphi(\tau) = \varphi(\tau)$.

Definition 2.2 ([11, 16])**.** The Caputo derivative of a function $\varphi : [0, 1) \to \mathbb{R}$, of order ρ within $0 < \rho < 1$, is defined as:

$$D^\rho \varphi(\tau) = \frac{1}{\Gamma(1-\rho)} \int_0^\tau \frac{\varphi^{(0)}(\aleph)}{(\tau - \aleph)^\rho} d\aleph, \quad \tau > 0.$$

Here, $\Gamma(1-\rho)$ denotes the Gamma function evaluated at $1-\rho$, and $\varphi^{(0)}(\aleph)$ refers to the zeroth derivative (or the function φ itself).

Definition 2.3 ([11, 16])**.** For a function $\varphi(\tau)$, the Caputo fractional derivative is specified for an order ρ between $n-1$ and n, where $n \in \mathbb{N}$. It is given by:

$${}^cD^\rho \varphi(\tau) = \frac{1}{\Gamma(n-\rho)} \int_0^\tau (\tau - \aleph)^{n-\rho-1} \frac{d^n \varphi(\aleph)}{d\aleph^n} d\aleph, \quad n-1 < \rho < n.$$

When $\rho = n$, the fractional derivative reduces to the standard n-th order derivative:

$${}^cD^\rho \varphi(\tau) = \frac{d^n \varphi(\tau)}{d\tau^n}.$$

The order ρ in this context can be real or even complex, representing the derivative's fractional order.

Theorem 2.4. (Schauder fixed point theorem, see [10]) If a continuous mapping $N : B \to B$ has a relatively compact image in the Banach space E, then there exists at least one fixed point in the closed and convex subset B.

Theorem 2.5. (Arzelà-Ascoli theorem, see [11]) On a closed and bounded interval $[a, b]$, any sequence of functions that is equicontinuous and bounded must possess a subsequence that converges uniformly.

This work incorporates an axiomatic definition for the phase space $\mathcal{B}$, similar to the frameworks described in [29]. The phase space $\mathcal{B}$ is defined as a linear space consisting of all mappings from $(-\infty, 0]$ to X. It is equipped with a seminorm $\|\cdot\|_\mathcal{B}$, satisfying the following axioms.

(A1) Let $\eta : (-\infty, a] \to X$ be a function, where $a > 0$, continuous on J, and $\eta_0 \in \mathcal{B}$. For every $\aleph \in J$, the following properties hold:

(i) the function $\eta_\aleph$ belongs to $\mathcal{B}$;

(ii) $\|\eta(\aleph)\| \leqslant H\|\eta_\aleph\|_{\mathcal{B}}$;
(iii) $\|\eta_\aleph\|_{\mathcal{B}} \leqslant K(\aleph)\sup\{\|\eta(\xi)\| : 0 \leqslant \xi \leqslant \aleph\} + M(\aleph)\|\eta_0\|_{\mathcal{B}}$,
where $H > 0$ is a constant, $K : [0,\infty) \to [1,\infty)$ is a continuous function, $M : [0,\infty) \to [1,\infty)$ is locally bounded, and the parameters H, K, and M are independent of $\eta(\cdot)$.

(A2) For $\eta(\cdot)$ defined in (A1), the function $\eta_\aleph$ is continuous and takes values in $\mathcal{B}$ on J.

(A3) The space $\mathcal{B}$ is complete.

3. Controllability results for fractional VFIDE with SDD

This section focuses on defining the concept of a mild solution for fractional VFIDEs with SDD, as represented in equations (1.1). Building on the preceding discussion, we further explore the controllability of these mild solutions.

Definition 3.1. *A function $\eta : (-\infty, b] \to X$ is considered a mild solution of equations (1.1) if it satisfies $\eta_0 = \varphi \in \mathcal{B}$ for all $\sigma, \aleph \in J$,*

$$\begin{aligned}\eta(\aleph) = {} & S_\rho(\aleph)\,\eta_0 + \int_{\aleph_0}^{\aleph} T_\rho(\aleph-\sigma)\,(\aleph-\sigma)^{\rho-1} g(\sigma, \eta_{\rho(\aleph,\eta_s)})\,d\sigma \\ & + \int_{\aleph_0}^{\aleph} T_\rho(\aleph-\sigma)\,(\aleph-\sigma)^{\rho-1} \int_\sigma^{\aleph} Z_1(\tau,\sigma,\eta_{\rho(\aleph,\eta_s)})\,d\tau d\sigma \\ & + \int_{\aleph_0}^{\aleph} T_\rho(\aleph-\sigma)\,(\aleph-\sigma)^{\rho-1} \int_\sigma^{b} Z_2(\tau,\sigma,\eta_{\rho(\aleph,\eta_s)})\,d\tau d\sigma + \int_{\aleph_0}^{\aleph} T_\rho(\aleph-\sigma)\,(\aleph-\sigma)^{\rho-1} B(\sigma)u(\sigma)\,d\sigma,\end{aligned} \tag{3.1}$$

where

$$S_\rho(\aleph) = \int_0^\infty \phi_\rho(\theta) T(\aleph^\rho\theta)\,d\theta, \qquad T_\rho(\aleph) = \rho\int_0^\infty \theta\phi_\rho(\theta) T(\aleph^\rho\theta)\,d\theta,$$

$$\phi_\rho(\theta) = \frac{1}{\rho}\theta^{-1-\frac{1}{\rho}}\psi_\rho(\theta^{-\frac{1}{\rho}}), \qquad \psi_\rho(\theta) = \frac{1}{\pi}\sum_{n=1}^{\infty}(-1)^{n-1}\theta^{-\rho n-1}\frac{\Gamma(n\rho+1)}{n!}\sin(n\pi\rho), \quad \theta \in (0,\infty),$$

and ϕ_ρ is a probability density function defined on $(0,\infty)$, which means $\phi_\rho(\theta) \geqslant 0$, $\theta \in (0,\infty)$, and $\int_0^\infty \phi_\rho(\theta)\,d\theta = 1$.

Lemma 3.2 ([26]). *For any $\aleph \geqslant 0$, the operators $S_\rho(\aleph)$ and $T_\rho(\aleph)$ have the following properties.*

(a) For each fixed $\aleph \geqslant 0$, S_ρ and T_ρ are linear and bounded operators. Specifically, for any $\eta \in X$,

$$\|S_\rho(\aleph)\eta\| \leqslant M\|\eta\|, \quad \|T_\rho(\aleph)\eta\| \leqslant \frac{\rho M}{\Gamma(1+\rho)}\|\eta\|.$$

(b) The families $\{S_\rho(\aleph) : \aleph \geqslant 0\}$ and $\{T_\rho(\aleph) : \aleph \geqslant 0\}$ are strongly continuous.
(c) For each $\aleph > 0$, the operators $S_\rho(\aleph)$ and $T_\rho(\aleph)$ are compact.

Definition 3.3. *The system described by equations (1.1) is deemed controllable over the interval J if there exists a control function $\delta(\aleph)$ in the space $L^2(J,U)$. For any initial states η_0 and η_1 in the Banach space X, this control function ensures that the mild solution $\eta(\aleph)$ satisfies $\eta(\aleph_0) = \eta_0$ and $\eta(b) = \eta_1$.*

To derive our results, we consistently assume that $\rho : J \times \mathcal{B} \to (-\infty, b]$ is a continuous function. In addition, the following conditions are introduced.

(H1) For all $\aleph > 0$, the semigroup $T(\aleph)$ is compact.

(H2) The function $g : J \times \mathcal{B} \to X$ is continuous, and there exist constants $L_g > 0$ and $L_g^* > 0$ such that the following inequality holds for all $\aleph \in J$ and $(\vartheta, \vartheta_1) \in \mathcal{B}^2$:

$$\|g(\aleph, \vartheta) - g(\aleph, \vartheta_1)\|_X \leqslant L_g \|\vartheta - \vartheta_1\|_{\mathcal{B}}.$$

Additionally, the constant L_g^* is defined as $L_g^* = \max_{\aleph \in J} \|g(\aleph, 0)\|_X$.

(H3) The functions $Z_i : D \times \mathcal{B} \to X$ for $i = 1, 2$ are continuous, and there exist constants $L_{Z_i} > 0$ and $L_{Z_i}^* > 0$ such that the following inequalities hold for $(\aleph, \sigma) \in D$ and $(\vartheta, \vartheta_1) \in \mathcal{B}^2$:

$$\|Z_1(\aleph, \sigma, \vartheta) - Z_1(\aleph, \sigma, \vartheta_1)\|_X \leqslant L_{Z_1} \|\vartheta - \vartheta_1\|_{\mathcal{B}}, \quad \|Z_2(\aleph, \sigma, \vartheta) - Z_2(\aleph, \sigma, \vartheta_1)\|_X \leqslant L_{Z_2} \|\vartheta - \vartheta_1\|_{\mathcal{B}}.$$

Additionally, we define

$$L_{Z_1^*} = \max_{\aleph, \sigma \in D} \|Z_1(\aleph, \sigma, 0)\|_X, \quad L_{Z_2^*} = \max_{\aleph, \sigma \in D} \|Z_2(\aleph, \sigma, 0)\|_X.$$

(H4) The function $\aleph \to \varphi_t$ is well-defined and continuous, mapping from the set $R(\rho^-) = \{\rho(\sigma, \vartheta) : (\sigma, \vartheta) \in J \times \mathcal{B}, \rho(\sigma, \vartheta) \leqslant 0\}$ into $\mathcal{B}$. Furthermore, there exists a continuous and bounded function $J^\varphi : R(\rho^-) \to (0, \infty)$ such that for every $\aleph \in R(\rho^-)$, the following inequality holds:

$$\|\varphi_t\|_{\mathcal{B}} \leqslant J^\varphi(\aleph) \|\varphi\|_{\mathcal{B}}.$$

(H5) The operator $W : L^2(J, U) \to X$ is a bounded linear operator, defined by

$$Wx = \frac{1}{\Gamma(\rho)} \int_{\aleph_0}^{b} (b - \aleph)^{\rho - 1} Bu(\aleph) d\aleph.$$

It has an induced inverse W^{-1}, which operates within the quotient space $\frac{L^2(J,U)}{\ker W}$. Additionally, there are positive constants M_1 and M_2 such that $|B| \leqslant M_1$ and $|W^{-1}| \leqslant M_2$.

Theorem 3.4. *If hypotheses* (H1)-(H5) *hold, the system described by equations* (1.1) *is controllable within the interval* $[\aleph_0, b]$.

Proof. Based on the assumptions provided in hypothesis (H5), we can establish a control derived from the properties of an arbitrary function $\eta(\cdot)$. Consider the set ϖ_l, which consists of all continuous functions η defined on an interval J and taking real values, subject to the condition $\|\eta\|_\infty \leqslant l$,

$$\begin{aligned} \mu(\aleph) = W^{-1} \Bigg[\eta_1 - S_\rho(\aleph)\, \eta_0 - \int_{\aleph_0}^{\aleph} T_\rho(\aleph - \sigma)\, (\aleph - \sigma)^{\rho - 1} \Bigg[g(\sigma, \eta_{\rho(\aleph, \eta_s)}) \\ + \int_\sigma^{\aleph} Z_1(\tau, \sigma, \eta_{\rho(\aleph, \eta_s)}) d\tau + \int_\sigma^{b} Z_2(\tau, \sigma, \eta_{\rho(\aleph, \eta_s)}) d\tau \Bigg] d\sigma \Bigg] (\aleph). \end{aligned} \tag{3.2}$$

The operator Φ, defined as mapping from the set ϖ_l to itself, will be demonstrated with the defined control to satisfy the necessary conditions,

$$\begin{aligned} \Phi(\eta)(\aleph) = S_\rho(\aleph)\, \eta_0 + \int_{\aleph_0}^{\aleph} T_\rho(\aleph - \sigma)(\aleph - \sigma)^{\rho - 1} g(\sigma, \eta_{\rho(\aleph, \eta_s)}) d\sigma \\ + \int_{\aleph_0}^{\aleph} T_\rho(\aleph - \sigma)(\aleph - \sigma)^{\rho - 1} \int_\sigma^{\aleph} Z_1(\tau, \sigma, \eta_{\rho(\aleph, \eta_s)}) d\tau d\sigma \\ + \int_{\aleph_0}^{\aleph} T_\rho(\aleph - \sigma)(\aleph - \sigma)^{\rho - 1} \int_\sigma^{b} Z_2(\tau, \sigma, \eta_{\rho(\aleph, \eta_s)}) d\tau d\sigma + \int_{\aleph_0}^{\aleph} T_\rho(\aleph - \sigma)(\aleph - \sigma)^{\rho - 1} B\mu(\sigma) d\sigma. \end{aligned} \tag{3.3}$$

Building upon equation (3.1), for any function η in the set ϖ_l and for all values of $\aleph$ within the interval $[\aleph_0, b]$, we can establish the following relationship. Since all the functions included in the operator's definition are continuous, we can conclude that the operator Φ is continuous.

We can also conclude that there exists a fixed point for the operator Φ, where $\mu(\aleph)$ is defined as per equation (3.3). This fixed point serves as the mild solution to the control problem described by equations (1.1). Specifically, it is evident that $\Phi\ \eta(b) = \eta_1$, which implies that the system represented by equations (1.1) is controllable over the interval $[\aleph_0, b]$,

$$\begin{aligned}
\mu(\aleph) &\leqslant \|W^{-1}\|\Bigg[\|\eta_1\| - \|S_\rho(\aleph)\|\|\eta_0\| - \int_{\aleph_0}^{\aleph} T_\rho(\aleph-\sigma)\ (\aleph-\sigma)^{\rho-1}\Bigg[\|g(\sigma,\eta_{\rho(\aleph,\eta_s)})\| \\
&\quad + \int_\sigma^{\aleph}\|Z_1(\tau,\sigma,\eta_{\rho(\aleph,\eta_s)})\|d\tau + \int_\sigma^{b}\|Z_2(\tau,\sigma,\eta_{\rho(\aleph,\eta_s)})\|d\tau\Bigg]d\sigma\Bigg] \\
&\leqslant M_2\Bigg[\|\eta_1\| + M\|\eta_0\| + \frac{\rho M}{\Gamma(1+\rho)}\int_{\aleph_0}^{\aleph}(\aleph-\sigma)^{\rho-1}\|g(\sigma,\eta_{\rho(\aleph,\eta_s)})\|d\sigma + \frac{\rho M}{\Gamma(1+\rho)}\int_{\aleph_0}^{\aleph}(\aleph-\sigma)^{\rho-1} \\
&\quad \times \int_\sigma^{\aleph}\|Z_1(\tau,\sigma,\eta_{\rho(\aleph,\eta_s)})\|d\tau\ d\sigma + \frac{\rho M}{\Gamma(1+\rho)}\int_{\aleph_0}^{\aleph}(\aleph-\sigma)^{\rho-1}\int_\sigma^{b}\|Z_2(\tau,\sigma,\eta_{\rho(\aleph,\eta_s)})\|d\tau\ d\sigma\Bigg] \\
&\leqslant M_2\Bigg[\|\eta_1\| + M\|\eta_0\| + \frac{\rho M}{\Gamma(1+\rho)}\int_{\aleph_0}^{\aleph}(\aleph-\sigma)^{\rho-1}\Bigg[L_g\|\eta_{\rho(\sigma,\bar{\eta_s})}\|_{\mathcal{B}} + L_g^* \\
&\quad + \int_\sigma^{\aleph}(L_{Z_1}\|\eta_{\rho(\sigma,\bar{\eta_s})}\|_{\mathcal{B}} + L_{Z_1}^*)d\tau + \int_\sigma^{b}(L_{Z_2}\|\eta_{\rho(\sigma,\bar{\eta_s})}\|_{\mathcal{B}} + L_{Z_2}^*)d\tau\Bigg]d\sigma\Bigg] \\
&\leqslant M_2\Bigg[\|\eta_1\| + M\|\eta_0\| + \frac{Me^\rho}{\Gamma(1+\rho)}\ (L_g r^* + L_g^*) + \frac{Me^{\rho+1}}{(\rho+1)\Gamma(\rho)}(L_{Z_1}r^* + L_{Z_1}^*) + \frac{Me^{\rho+1}}{(\rho+1)\Gamma(\rho)}(L_{Z_2}r^* + L_{Z_2}^*)\Bigg] \\
&\leqslant M_2\Bigg[\|\eta_1\| + M\|\eta_0\| + Me^\rho\left[\frac{L_g}{\Gamma(\rho+1)} + \frac{e(L_{Z_1}+L_{Z_2})}{(\rho+1)\Gamma(\rho)}\right]r^* + Me^\rho\left[\frac{L_g^*}{\Gamma(\rho+1)} + \frac{e(L_{Z_1}^*+L_{Z_2}^*)}{(\rho+1)\Gamma(\rho)}\right]\Bigg].
\end{aligned}$$

Applying the equations (3.2) and (3.3), we can derive the subsequent result:

$$\begin{aligned}
\|\Phi(\eta)(\aleph)\| &\leqslant M\|\eta_0\| + \frac{\rho M}{\Gamma(1+\rho)}\int_{\aleph_0}^{\aleph}(\aleph-\sigma)^{\rho-1}\|g(\sigma,\eta_{\rho(\aleph,\eta_s)})\|d\sigma + \frac{\rho M}{\Gamma(1+\rho)}\int_{\aleph_0}^{\aleph}(\aleph-\sigma)^{\rho-1} \\
&\quad \times \int_\sigma^{\aleph}\|Z_1(\tau,\sigma,\eta_{\rho(\aleph,\eta_s)})\|d\tau\ d\sigma + \frac{\rho M}{\Gamma(1+\rho)}\int_{\aleph_0}^{\aleph}(\aleph-\sigma)^{\rho-1}\int_\sigma^{b}\|Z_2(\tau,\sigma,\eta_{\rho(\aleph,\eta_s)})\|d\tau\ d\sigma \\
&\quad + \frac{\rho M}{\Gamma(1+\rho)}\int_{\aleph_0}^{\aleph}(\aleph-\sigma)^{\rho-1}\|B\|\|\mu(\aleph)\| \\
&\leqslant M\|\eta_0\| + \frac{\rho M}{\Gamma(1+\rho)}\int_{\aleph_0}^{\aleph}(\aleph-\sigma)^{\rho-1}\Bigg[L_g\|\eta_{\rho(\sigma,\bar{\eta_s})}\|_{\mathcal{B}} + L_g^* + \int_\sigma^{\aleph}(L_{Z_1}\|\eta_{\rho(\sigma,\bar{\eta_s})}\|_{\mathcal{B}} + L_{Z_1}^*)d\tau \\
&\quad + \int_\sigma^{b}(L_{Z_2}\|\eta_{\rho(\sigma,\bar{\eta_s})}\|_{\mathcal{B}} + L_{Z_2}^*)d\tau\Bigg]d\sigma + \frac{\rho M}{\Gamma(1+\rho)}\int_{\aleph_0}^{\aleph}(\aleph-\sigma)^{\rho-1}M_1\|\mu(\aleph)\| \\
&\leqslant M\|\eta_0\| + \frac{Me^\rho}{\Gamma(1+\rho)}\ (L_g r^* + L_g^*) + \frac{Me^{\rho+1}}{(\rho+1)\Gamma(\rho)}(L_{Z_1}r^* + L_{Z_1}^*) \\
&\quad + \frac{Me^{\rho+1}}{(\rho+1)\Gamma(\rho)}(L_{Z_2}r^* + L_{Z_2}^*) + \frac{Me^\rho}{\Gamma(1+\rho)}\ M_1M_2\Bigg[\|\eta_1\| - M\|\eta_0\| \\
&\quad + \frac{Me^\rho}{\Gamma(1+\rho)}\ (L_g r^* + L_g^*) + \frac{Me^{\rho+1}}{(\rho+1)\Gamma(\rho)}(L_{Z_1}r^* + L_{Z_1}^*) + \frac{Me^{\rho+1}}{(\rho+1)\Gamma(\rho)}(L_{Z_2}r^* + L_{Z_2}^*)\Bigg]
\end{aligned}$$

$$\leqslant M\|\eta_0\| + Me^{\rho}\left[\frac{L_g}{\Gamma(\rho+1)} + \frac{e(L_{Z_1}+L_{Z_2})}{(\rho+1)\Gamma(\rho)}\right]r^* + Me^{\rho}\left[\frac{L_g^*}{\Gamma(\rho+1)} + \frac{e(L_{Z_1}^*+L_{Z_2}^*)}{(\rho+1)\Gamma(\rho)}\right]$$
$$+ \frac{Me^{\rho}}{\Gamma(1+\rho)}\, M_1M_2\left[\|\eta_1\| + M\|\eta_0\| + Me^{\rho}\left[\frac{L_g}{\Gamma(\rho+1)} + \frac{e(L_{Z_1}+L_{Z_2})}{(\rho+1)\Gamma(\rho)}\right]r^*\right.$$
$$\left. + Me^{\rho}\left[\frac{L_g^*}{\Gamma(\rho+1)} + \frac{e(L_{Z_1}^*+L_{Z_2}^*)}{(\rho+1)\Gamma(\rho)}\right]\right]$$
$$\leqslant \frac{Me^{\rho}}{\Gamma(1+\rho)}\, M_1M_2\|\eta_1\| + \left(1 + \frac{Me^{\rho}}{\Gamma(1+\rho)}\, M_1M_2\right)\left[M\|\eta_0\| + Me^{\rho}\left[\frac{L_g}{\Gamma(\rho+1)} + \frac{e(L_{Z_1}+L_{Z_2})}{(\rho+1)\Gamma(\rho)}\right]r^*\right.$$
$$\left. + Me^{\rho}\left[\frac{L_g^*}{\Gamma(\rho+1)} + \frac{e(L_{Z_1}^*+L_{Z_2}^*)}{(\rho+1)\Gamma(\rho)}\right]\right].$$

Thus,

$$\|\Phi(\eta)\|_\infty \leqslant \frac{Me^{\rho}}{\Gamma(1+\rho)}\, M_1M_2\|\eta_1\| + \left(1 + \frac{Me^{\rho}}{\Gamma(1+\rho)}\, M_1M_2\right)\left[M\|\eta_0\| + Me^{\rho}\left[\frac{L_g}{\Gamma(\rho+1)} + \frac{e(L_{Z_1}+L_{Z_2})}{(\rho+1)\Gamma(\rho)}\right]r^*\right.$$
$$\left. + Me^{\rho}\left[\frac{L_g^*}{\Gamma(\rho+1)} + \frac{e(L_{Z_1}^*+L_{Z_2}^*)}{(\rho+1)\Gamma(\rho)}\right]\right] := l.$$

Therefore, we conclude that $\|\Phi\eta\| \leqslant l$, meaning $\Phi\eta$ belongs to ϖ_l. This leads to the conclusion that $\Phi\varpi_l \subset \varpi_l$.

We will now proceed to demonstrate that the operator $\Phi : \varpi_l \to \varpi_l$ satisfies all the requirements of (2.4). This will be proven in multiple steps. First, we show that the operator Φ maps the set $\varpi_l = \{\eta \in C(J,X) : \|\eta\|_\infty \leqslant l\}$ onto itself.

Step 1: Continuity of Φ. Let η_n be a sequence such that $\eta_n \to \eta$ in ϖ_l,

$$\|\Phi\eta_n(\aleph) - \Phi\eta(\aleph)\| \leqslant \int_{\aleph_0}^{\aleph} T_\rho(\aleph-\sigma)(\aleph-\sigma)^{\rho-1}\|g(\sigma,\eta_{n\rho(\aleph,\eta_s)}) - g(\sigma,\eta_{\rho(\aleph,\eta_s)})\|d\sigma$$
$$+ \int_{\aleph_0}^{\aleph} T_\rho(\aleph-\sigma)(\aleph-\sigma)^{\rho-1}\int_\sigma^{\aleph}\|Z_1(\tau,\sigma,\eta_{n\rho(\aleph,\eta_s)}) - Z_1(\tau,\sigma,\eta_{\rho(\aleph,\eta_s)})\|d\tau d\sigma$$
$$+ \int_{\aleph_0}^{\aleph} T_\rho(\aleph-\sigma)(\aleph-\sigma)^{\rho-1}\int_\sigma^{b}\|Z_2(\tau,\sigma,\eta_{n\rho(\aleph,\eta_s)}) - Z_2(\tau,\sigma,\eta_{\rho(\aleph,\eta_s)})\|d\tau d\sigma$$
$$+ \int_{\aleph_0}^{\aleph} T_\rho(\aleph-\sigma)(\aleph-\sigma)^{\rho-1}BW^{-1}\left[-\int_{\aleph_0}^{\aleph} T_\rho(\aleph-\sigma)(\aleph-\sigma)^{\rho-1}\|g(\sigma,\eta_{n\rho(\aleph,\eta_s)})\right.$$
$$- g(\sigma,\eta_{\rho(\aleph,\eta_s)})\|d\sigma + \int_{\aleph_0}^{\aleph} T_\rho(\aleph-\sigma)(\aleph-\sigma)^{\rho-1}\int_\sigma^{\aleph}\|Z_1(\tau,\sigma,\eta_{n\rho(\aleph,\eta_s)})$$
$$- Z_1(\tau,\sigma,\eta_{\rho(\aleph,\eta_s)})\|d\tau d\sigma + \int_{\aleph_0}^{\aleph} T_\rho(\aleph-\sigma)(\aleph-\sigma)^{\rho-1}\int_\sigma^{b}\|Z_2(\tau,\sigma,\eta_{n\rho(\aleph,\eta_s)})$$
$$\left. - Z_2(\tau,\sigma,\eta_{\rho(\aleph,\eta_s)})\|d\tau d\sigma\right]d\sigma.$$

Since g, Z_1, and Z_2 are continuous, it follows that $\|\Phi\eta_n(\aleph) - \Phi\eta(\aleph)\| \to 0$ as $n \to \infty$. Hence, Φ is continuous on the set ϖ_l.

Step 2: The set $\Phi(\varpi_l)$ is uniformly bounded, as it is a subset of ϖ_l, which ensures its boundedness.

Step 3: We establish the equicontinuity of the set $\Phi(\varpi_l)$.

Consider $\aleph_1$ and $\aleph_2$ belonging to the bounded set $[\aleph_0, b]$ in $C(J, X)$ as in Step 2, along with η from ϖ_l and $\aleph_1 < \aleph_2$. In this context, we have

$$
\begin{aligned}
&\|(\Phi\eta)(\aleph_2) - (\Phi\eta)(\aleph_1)\| \\
&= \Bigg\| S_\rho(\aleph_2)\ \eta_0 + \int_{\aleph_0}^{\aleph_2} T_\rho(\aleph_2-\sigma)(\aleph_2-\sigma)^{\rho-1} g(\sigma, \eta_{\rho(\sigma,\eta_s)})\,d\sigma \\
&\quad + \int_{\aleph_0}^{\aleph_2} (\aleph_2-\sigma)^{\rho-1} T_\rho(\aleph_2-\sigma) \int_\sigma^{\aleph_2} Z_1(\tau, \sigma, \eta_{\rho(\sigma,\eta_s)})\,d\tau d\sigma \\
&\quad + \int_{\aleph_0}^{\aleph_2} (\aleph_2-\sigma)^{\rho-1} T_\rho(\aleph_2-\sigma) \int_\sigma^{b} Z_2(\tau, \sigma, \eta_{\rho(\sigma,\eta_s)})\,d\tau d\sigma \\
&\quad + \int_{\aleph_0}^{\aleph_2} (\aleph_2-\sigma)^{\rho-1} T_\rho(\aleph_2-\sigma) BW^{-1} \Bigg[\eta_1 - S_\rho(\aleph_2)\ \eta_0 - \int_{\aleph_0}^{\aleph_2} T_\rho(\aleph_2-\sigma)\ (\aleph_2-\sigma)^{\rho-1} \Bigg[g(\sigma, \eta_{\rho(\sigma,\eta_s)}) \\
&\quad + \int_\sigma^{\aleph_2} Z_1(\tau, \sigma, \eta_{\rho(\aleph_2,\eta_s)})\,d\tau + \int_\sigma^{b} Z_2(\tau, \sigma, \eta_{\rho(\aleph_2,\eta_s)})\,d\tau \Bigg] d\sigma \Bigg] \\
&\quad - S_\rho(\aleph_1)\ \eta_0 - \int_{\aleph_0}^{\aleph_1} T_\rho(\aleph_1-\sigma)(\aleph_1-\sigma)^{\rho-1} g(\sigma, \eta_{\rho(\sigma,\eta_s)})\,d\sigma \\
&\quad - \int_{\aleph_0}^{\aleph_1} (\aleph_1-\sigma)^{\rho-1} T_\rho(\aleph_1-\sigma) \int_\sigma^{\aleph_1} Z_1(\tau, \sigma, \eta_{\rho(\sigma,\eta_s)})\,d\tau d\sigma \\
&\quad - \int_{\aleph_0}^{\aleph_1} (\aleph_1-\sigma)^{\rho-1} T_\rho(\aleph_1-\sigma) \int_\sigma^{b} Z_2(\tau, \sigma, \eta_{\rho(\sigma,\eta_s)})\,d\tau d\sigma \\
&\quad - \int_{\aleph_0}^{\aleph_1} (\aleph_1-\sigma)^{\rho-1} T_\rho(\aleph_1-\sigma) BW^{-1} \Bigg[\eta_1 - S_\rho(\aleph_1)\ \eta_0 - \int_{\aleph_0}^{\aleph_1} T_\rho(\aleph_1-\sigma)\ (\aleph_1-\sigma)^{\rho-1} \Bigg[g(\sigma, \eta_{\rho(\sigma,\eta_s)}) \\
&\quad + \int_\sigma^{\aleph_1} Z_1(\tau, \sigma, \eta_{\rho(\aleph_1,\eta_s)})\,d\tau + \int_\sigma^{b} Z_2(\tau, \sigma, \eta_{\rho(\aleph_1,\eta_s)})\,d\tau \Bigg] d\sigma \Bigg] \Bigg\| \\
&\leqslant \frac{M\rho}{\Gamma(1+\rho)} \Bigg\| \int_{\aleph_1}^{\aleph_2} (\aleph_2-\sigma)^{\rho-1} g(\sigma, \eta_{\rho(\sigma,\eta_s)})\,d\sigma + \int_{\aleph_1}^{\aleph_2} (\aleph_2-\sigma)^{\rho-1} \int_\sigma^{\aleph_2} Z_1(\tau, \sigma, \eta_{\rho(\sigma,\eta_s)})\,d\tau d\sigma \\
&\quad + \int_{\aleph_1}^{\aleph_2} (\aleph_2-\sigma)^{\rho-1} \int_\sigma^{b} Z_2(\tau, \sigma, \eta_{\rho(\sigma,\eta_s)})\,d\tau d\sigma - \int_{\aleph_0}^{\aleph_1} (\aleph_1-\sigma)^{\rho-1} g(\sigma, \eta_{\rho(\sigma,\eta_s)})\,d\sigma \\
&\quad - \int_{\aleph_0}^{\aleph_1} (\aleph_1-\sigma)^{\rho-1} \int_\sigma^{\aleph_1} Z_1(\tau, \sigma, \eta_{\rho(\sigma,\eta_s)})\,d\tau d\sigma - \int_{\aleph_0}^{\aleph_1} (\aleph_1-\sigma)^{\rho-1} \int_\sigma^{b} Z_2(\tau, \sigma, \eta_{\rho(\sigma,\eta_s)})\,d\tau d\sigma \\
&\quad + \int_{\aleph_0}^{\aleph_1} (\aleph_2-\sigma)^{\rho-1} g(\sigma, \eta_{\rho(\sigma,\eta_s)})\,d\sigma + \int_{\aleph_0}^{\aleph_1} (\aleph_2-\sigma)^{\rho-1} \int_\sigma^{\aleph_2} Z_1(\tau, \sigma, \eta_{\rho(\sigma,\eta_s)})\,d\tau d\sigma \\
&\quad + \int_{\aleph_0}^{\aleph_1} (\aleph_2-\sigma)^{\rho-1} \int_\sigma^{b} Z_2(\tau, \sigma, \eta_{\rho(\sigma,\eta_s)})\,d\tau d\sigma + BW^{-1} \Bigg[\int_{\aleph_1}^{\aleph_2} (\aleph_2-\sigma)^{\rho-1} g(\sigma, \eta_{\rho(\sigma,\eta_s)})\,d\sigma \\
&\quad + \int_{\aleph_1}^{\aleph_2} (\aleph_2-\sigma)^{\rho-1} \int_\sigma^{\aleph_2} Z_1(\tau, \sigma, \eta_{\rho(\sigma,\eta_s)})\,d\tau d\sigma + \int_{\aleph_1}^{\aleph_2} (\aleph_2-\sigma)^{\rho-1} \int_\sigma^{b} Z_2(\tau, \sigma, \eta_{\rho(\sigma,\eta_s)})\,d\tau d\sigma \\
&\quad - \int_{\aleph_0}^{\aleph_1} (\aleph_1-\sigma)^{\rho-1} g(\sigma, \eta_{\rho(\sigma,\eta_s)})\,d\sigma - \int_{\aleph_0}^{\aleph_1} (\aleph_1-\sigma)^{\rho-1} \int_\sigma^{\aleph_1} Z_1(\tau, \sigma, \eta_{\rho(\sigma,\eta_s)})\,d\tau d\sigma \\
&\quad - \int_{\aleph_0}^{\aleph_1} (\aleph_1-\sigma)^{\rho-1} \int_\sigma^{b} Z_2(\tau, \sigma, \eta_{\rho(\sigma,\eta_s)})\,d\tau d\sigma + \int_{\aleph_0}^{\aleph_1} (\aleph_2-\sigma)^{\rho-1} g(\sigma, \eta_{\rho(\sigma,\eta_s)})\,d\sigma
\end{aligned}
$$

$$
\begin{aligned}
&+\int_{\aleph_0}^{\aleph_1}(\aleph_2-\sigma)^{\rho-1}\int_{\sigma}^{\aleph_2}Z_1(\tau,\sigma,\eta_{\rho(\sigma,\eta_s)})d\tau d\sigma+\int_{\aleph_0}^{\aleph_1}(\aleph_2-\sigma)^{\rho-1}\int_{\sigma}^{b}Z_2(\tau,\sigma,\eta_{\rho(\sigma,\eta_s)})d\tau d\sigma\Bigg]\Bigg\|\\
&\leqslant\frac{M\rho}{\Gamma(1+\rho)}\Bigg\|\int_{\aleph_1}^{\aleph_2}(\aleph_2-\sigma)^{\rho-1}\Bigg[g(\sigma,\eta_{\rho(\sigma,\eta_s)})+\int_{\sigma}^{\aleph_2}Z_1(\tau,\sigma,\eta_{\rho(\sigma,\eta_s)})d\tau+\int_{\sigma}^{b}Z_2(\tau,\sigma,\eta_{\rho(\sigma,\eta_s)})d\tau\Bigg]d\sigma\\
&-\int_{\aleph_0}^{\aleph_1}(\aleph_1-\sigma)^{\rho-1}g(\sigma,\eta_{\rho(\sigma,\eta_s)})d\sigma+\int_{\aleph_0}^{\aleph_1}(\aleph_2-\sigma)^{\rho-1}g(\sigma,\eta_{\rho(\sigma,\eta_s)})d\sigma\\
&-\int_{\aleph_0}^{\aleph_1}\Bigg[(\aleph_1-\sigma)^{\rho-1}\int_{\sigma}^{\aleph_1}Z_1(\tau,\sigma,\eta_{\rho(\sigma,\eta_s)})d\tau\\
&-(\aleph_2-\sigma)^{\rho-1}\int_{\sigma}^{\aleph_2}Z_1(\tau,\sigma,\eta_{\rho(\sigma,\eta_s)})d\tau\Bigg]d\sigma-\int_{\aleph_0}^{\aleph_1}\Bigg[(\aleph_1-\sigma)^{\rho-1}\\
&\times\int_{\sigma}^{b}Z_2(\tau,\sigma,\eta_{\rho(\sigma,\eta_s)})d\tau-(\aleph_2-\sigma)^{\rho-1}\int_{\sigma}^{b}Z_2(\tau,\sigma,\eta_{\rho(\sigma,\eta_s)})d\tau\Bigg]d\sigma\\
&+BW^{-1}\Bigg[\int_{\aleph_1}^{\aleph_2}(\aleph_2-\sigma)^{\rho-1}\Bigg[g(\sigma,\eta_{\rho(\sigma,\eta_s)})+\int_{\sigma}^{\aleph_2}Z_1(\tau,\sigma,\eta_{\rho(\sigma,\eta_s)})d\tau+\int_{\sigma}^{b}Z_2(\tau,\sigma,\eta_{\rho(\sigma,\eta_s)})d\tau\Bigg]d\sigma\\
&-\int_{\aleph_0}^{\aleph_1}(\aleph_1-\sigma)^{\rho-1}g(\sigma,\eta_{\rho(\sigma,\eta_s)})d\sigma+\int_{\aleph_0}^{\aleph_1}(\aleph_2-\sigma)^{\rho-1}g(\sigma,\eta_{\rho(\sigma,\eta_s)})d\sigma\\
&-\int_{\aleph_0}^{\aleph_1}\Bigg[(\aleph_1-\sigma)^{\rho-1}\int_{\sigma}^{\aleph_1}Z_1(\tau,\sigma,\eta_{\rho(\sigma,\eta_s)})d\tau\\
&-(\aleph_2-\sigma)^{\rho-1}\int_{\sigma}^{\aleph_2}Z_1(\tau,\sigma,\eta_{\rho(\sigma,\eta_s)})d\tau\Bigg]d\sigma-\int_{\aleph_0}^{\aleph_1}\Bigg[(\aleph_1-\sigma)^{\rho-1}\\
&\times\int_{\sigma}^{b}Z_2(\tau,\sigma,\eta_{\rho(\sigma,\eta_s)})d\tau-(\aleph_2-\sigma)^{\rho-1}\int_{\sigma}^{b}Z_2(\tau,\sigma,\eta_{\rho(\sigma,\eta_s)})d\tau\Bigg]d\sigma\Bigg]\Bigg\|.
\end{aligned}
$$

As $\aleph_2-\aleph_1\to 0$, the right-hand side approaches zero. The strong continuity of the semigroup $T_\rho(\aleph)$ for $\aleph\geqslant 0$, combined with its compactness for $\aleph>0$ (which ensures that $T_\rho(\aleph)$ is continuous in the uniform operator topology for $\aleph>0$), implies the equicontinuity in these cases. The same reasoning straightforwardly applies for the scenarios where $\aleph_1<\aleph_2\leqslant 0$ or $\aleph_1\leqslant 0\leqslant\aleph_2\leqslant b$.

By combining the results of Steps 1-3 and applying Theorem 2.5, we confirm the continuity and compactness of the operator Φ. From Theorem 2.4, we then conclude the existence of a fixed point η, which serves as a solution to the system described by equations (1.1). Consequently, this proves that the system is controllable on the interval $J=[\aleph_0,b]$, thereby completing the proof of the theorem. □

4. Example

As an illustrative example, we examine a control system governed by fractional VFIDEs with SDD of the following form:

$$
\begin{aligned}
{}^{c}D^{\rho}x(\aleph,\eta)=\frac{\partial^2}{\partial\eta^2}\Bigg[&x(\aleph,\eta)+\mu(\aleph,\eta)+\int_{-\infty}^{\aleph}\frac{e^{2(\sigma-\aleph)}x(\sigma-\rho_1(\sigma)\rho_2(\|x(\sigma)\|),u)}{64}d\sigma\\
&+\int_{-\infty}^{\aleph}\frac{e^{2(\tau-\sigma)}x(\tau-\rho_1(\tau)\rho_2(\|x(\tau)\|),\eta)}{16}d\tau d\sigma\\
&+\int_{0}^{\aleph}\sin(\aleph-\sigma)\int_{-\infty}^{\sigma}\frac{e^{2(\tau-\sigma)}x(\tau-\rho_1(\tau)\rho_2(\|x(\tau)\|),\eta)}{36}d\tau d\sigma\\
&+\int_{0}^{\aleph}\sin(\aleph-\sigma)\int_{-\infty}^{\sigma}\frac{e^{2(\tau-\sigma)}x(\tau-\rho_1(\tau)\rho_2(\|x(\tau)\|),\eta)}{36}d\tau d\sigma\Bigg]
\end{aligned}
\tag{4.1}
$$

with boundary conditions

$$x(\aleph, 0) = 0 = x(\aleph, \pi), \quad \aleph \in [0, b], \tag{4.2}$$

and initial condition

$$x(\aleph, \eta) = \varphi(\aleph, \eta), \quad \aleph \leqslant 0, \quad \eta \in [0, \pi]. \tag{4.3}$$

Let $X = L^2[0,\pi]$ with the L^2-norm $\|\cdot\|_{L^2}$. Consider the Caputo derivative ${}^cD_t^\rho$ of order $(0,1)$, and let $\varphi \in \mathcal{B}$. The operator $\mathcal{A} : D(\mathcal{A}) \subset X \to X$ is defined by $\mathcal{A}\zeta = \zeta''$, where the domain $D(\mathcal{A})$ consists of functions $\zeta \in X$ that satisfy: both ζ and ζ' are absolutely continuous, $\zeta'' \in X$, and the boundary conditions $\zeta(0) = \zeta(\pi) = 0$ are satisfied. The operator $\mathcal{A}\zeta$ can be written as:

$$\mathcal{A}\zeta = \sum_{n=1}^{\infty} n^2 \langle \zeta, \zeta_n \rangle \zeta_n, \quad \text{for } \zeta \in D(\mathcal{A}),$$

where the functions $\zeta_n(\sigma) = \sqrt{\frac{2}{\pi}} \sin(ns)$, for $n = 1, 2, \ldots$, form an orthonormal basis of eigenfunctions of $\mathcal{A}$. It is well-known that $\mathcal{A}$ generates an analytic semigroup $\{T(\aleph)\}_{\aleph \geqslant 0}$ in X, defined as:

$$T(\aleph)\zeta = \sum_{n=1}^{\infty} e^{-n^2\aleph} \langle \zeta, \zeta_n \rangle \zeta_n, \text{ for all } \zeta \in X \text{ and } \aleph > 0.$$

Since the semigroup $\{T(\aleph)\}_{\aleph \geqslant 0}$ is compact, there exists a constant $M > 0$ such that $\|T(\aleph)\|_{L(X)} \leqslant M$. For the phase space, we choose $x = e^{2s}$ for $\sigma < 0$, leading to $l = \int_{-\infty}^{0} x(\sigma) d\sigma = \frac{1}{2} < \infty$ for $\aleph \leqslant 0$. We then define the norm:

$$\|\zeta\|_{\mathcal{B}} = \int_{-\infty}^{0} x(\sigma) \sup_{\theta \in [\sigma, 0]} \|\zeta(\theta)\|_{L^2} d\sigma.$$

Thus, for $(\aleph, \varphi) \in [0, b] \times \mathcal{B}$, where $\varphi(\theta)(\eta) = \varphi(\theta, \eta)$ for $(\theta, \eta) \in (-\infty, 0] \times [0, \pi]$, we define $x(\aleph)(\eta) = x(\aleph, \eta)$ and $\rho(\aleph, \varphi) = \rho_1(\aleph)\rho_2(\|\varphi(0)\|)$. Consequently, we have:

$$\begin{aligned}
g(\aleph, \varphi)(\eta) &= \int_{-\infty}^{0} e^{2(\sigma)} \frac{\varphi}{16} d\sigma, \\
\int_0^{\aleph} Z_1(\aleph, \sigma, \varphi)(\eta) d\sigma &= \int_0^{\aleph} \sin(\aleph - \sigma) \int_{-\infty}^{0} e^{2(\sigma)} \frac{\varphi}{36} d\sigma, \\
\int_0^{\aleph} Z_2(\aleph, \sigma, \varphi)(\eta) d\sigma &= \int_0^{\aleph} \sin(\aleph - \sigma) \int_{-\infty}^{0} e^{2(\sigma)} \frac{\varphi}{16} d\sigma.
\end{aligned}$$

The system described by equations (4.1)-(4.3) can be formulated in the theoretical framework of equations (1.1) using these configurations. To analyze the system, we assume that the functions $\rho_i : [0, \infty) \to [0, \infty)$ for $i = 1, 2$ are continuous. Therefore, for $\aleph \in [0, T]$ and $\varphi, \bar{\varphi} \in \mathcal{B}$, the following conditions are satisfied:

$$\begin{aligned}
\|g(\aleph, \varphi) - g(\aleph, \bar{\varphi})\|_X &\leqslant \left(\int_0^{\pi} \left(\int_{-\infty}^{0} e^{2(\sigma)} \left\| \frac{\varphi}{16} - \frac{\bar{\varphi}}{16} \right\| d\sigma \right)^2 \right)^{\frac{1}{2}} \\
&\leqslant \left(\int_0^{\pi} \left(\frac{1}{16} \int_{-\infty}^{0} e^{2(\sigma)} \sup \|\varphi - \bar{\varphi}\| d\sigma \right)^2 \right)^{\frac{1}{2}} \leqslant \frac{\sqrt{\pi}}{16} \|\varphi - \bar{\varphi}\|_{\mathcal{B}} \leqslant L_g \|\varphi - \bar{\varphi}\|_{\mathcal{B}}, \\
\|Z_1(\aleph, \sigma, \varphi) - Z_1(\aleph, \sigma, \bar{\varphi})\|_X &\leqslant \left(\int_0^{\pi} \left(\int_{-\infty}^{0} e^{2(\sigma)} \left\| \frac{\varphi}{36} - \frac{\bar{\varphi}}{36} \right\| d\sigma \right)^2 \right)^{\frac{1}{2}} \\
&\leqslant \left(\int_0^{\pi} \left(\frac{1}{36} \int_{-\infty}^{0} e^{2(\sigma)} \sup \|\varphi - \bar{\varphi}\| d\sigma \right)^2 \right)^{\frac{1}{2}} \leqslant \frac{\sqrt{\pi}}{36} \|\varphi - \bar{\varphi}\|_{\mathcal{B}} \leqslant L_{Z_1} \|\varphi - \bar{\varphi}\|_{\mathcal{B}}.
\end{aligned}$$

Similarly, we can deduce that

$$\|Z_2(\aleph,\sigma,\varphi)-Z_2(\aleph,\sigma,\bar{\varphi})\|_X \leqslant \left(\int_0^{\pi}\left(\int_{-\infty}^{0} e^{2(\sigma)}\left\|\frac{\varphi}{16}-\frac{\bar{\varphi}}{16}\right\|d\sigma\right)^2\right)^{\frac{1}{2}}$$
$$\leqslant \left(\int_0^{\pi}\left(\frac{1}{16}\int_{-\infty}^{0} e^{2(\sigma)}\sup\|\varphi-\bar{\varphi}\|d\sigma\right)^2\right)^{\frac{1}{2}} \leqslant \frac{\sqrt{\pi}}{16}\|\varphi-\bar{\varphi}\|_{\mathcal{B}} \leqslant L_{Z_2}\|\varphi-\bar{\varphi}\|_{\mathcal{B}}.$$

Taking, $B : U \to X$ by $Bu(\aleph) = \mu(\aleph,\eta), 0 \leqslant \eta \leqslant \pi, u \in U$, where $\mu : [0,T]\times[0,\pi] \to X$ is continuous. Consequently, the conditions (H1)-(H5) are met. Additionally, assume that $M = 1, e = 1, r^* = \frac{1}{2}, L_g^*, L_{Z_1}^*, L_{Z_2}^* = 0.3$, and $\rho = \frac{1}{2}$. Then,

$$Me^{\rho}\left[\frac{L_g}{\Gamma(\rho+1)}+\frac{e(L_{Z_1}+L_{Z_2})}{(\rho+1)\Gamma(\rho)}\right]r^* = \frac{1}{2}\left(\frac{0.6611}{0.8655}+\frac{2(0.053+0.22)}{3}\right)+\left(\frac{0.5}{0.8655}+\frac{2}{3}\right)$$
$$= \frac{1}{2}(0.3154+0.2110)+0.6458+0.6888 = 0.7584 < 1.$$

Therefore, by Theorem 3.4, it is established that the equations (4.1)-(4.3) have a mild solution on $[0,1]$.

The numerical solution of the VFIDE is shown in Figure 1. Such an equation plays a significant role in modeling systems which contain memory effects and spatial interactions, as they appear in, for example, viscoelasticity, population dynamics, and diffusion-reaction systems. The mathematical structure combines a fractional derivative term with integral terms involving a kernel function, and this allows the equation to capture temporal and spatial dependencies simultaneously.

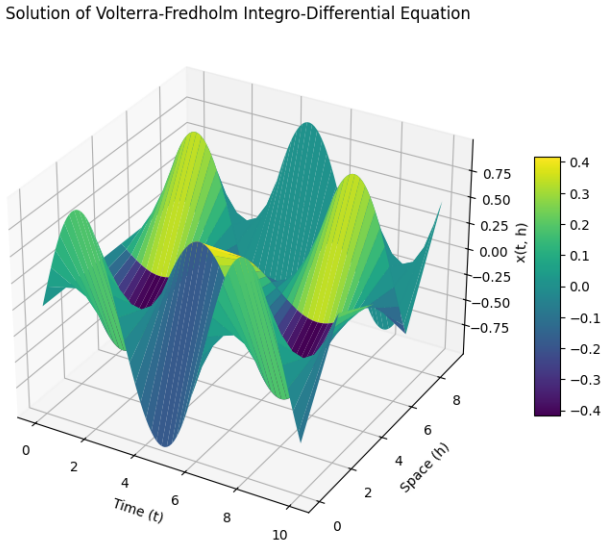

Figure 1: Numerical solution of the VFIDE showing the evolution of $x(\aleph,\eta)$ across time ($\aleph$) and space (η). The surface plot illustrates the periodic behavior induced by the source function and the smoothing effects of the kernel.

Figure 1 plots a graph of the solution $x(\aleph,\eta)$ in the temporal domain $[0,10]$ and the spatial domain $[0,9]$. The kernel function given by $\text{kernel}(\aleph,\eta,\sigma) = \beta e^{-(\aleph-\sigma)^2}\cos(\eta-\sigma)$ includes damping as well as oscillation effects since the temporal and spatial variables are now correlated. Again, the source function is given by

$$\text{source\_function}(\aleph,\eta) = \sin(\aleph)\cos(\eta),$$

which includes periodic forcing that initiates the oscillation of the solution. The periodic variations along the time axis can be seen from the surface plot. This corresponds to the sinusoidal nature of the source function. Along the spatial axis, oscillations are damped by the cosine term in the kernel. Contributions from earlier states are attenuated due to the exponential term in the kernel: $e^{-(\aleph-\sigma)^2}$, thus yielding a

continuous and well-behaved solution. The color gradient in the plot, as represented by the color bar, represents the magnitude of $x(\aleph, \eta)$. Bright regions correspond to higher values of the solution, while darker regions indicate lower values. The interplay between the source function and the kernel function results in the smooth yet complex patterns observed in the surface plot. This numerical simulation illustrates the ability of the VFIDE to model systems with distributed interactions and memory effects. The graph shows how the integral terms are incorporated into the dynamics of the system, involving past and spatially distributed information. Such behavior is particularly relevant in applications requiring the modeling of temporal delays and spatial interactions, such as in viscoelastic materials, biological systems, and wave propagation studies. The computation employed for this solution approximates integral terms using quadrature methods, ensuring precision in capturing the equation's non-local effects. Figure 1 presents an effective visualization of the solution and provides insight into the dynamics governed by the VFIDE.

5. Application of neural networks in controllability analysis

Here we discuss the controllability of mild solutions of a class of fractional VFIDEs with SDD governed by equations (1.1). In order to get past the obstacles provided by nonlinearity, fractional derivatives, and the presence of SDDs within the given equations, we consider using neural networks: more precisely, Physics-Informed Neural Networks (PINNs) in approximation of solutions for controllability conditions.

5.1. Neural network approach and parameterization of unknown functions

Physics-Informed Neural Networks (PINNs) exploit the dynamics of differential equations to enforce the governing equations of a given system throughout the training process. By incorporating fractional VFIDEs into the loss function of the neural network, it is ensured that the learned solution satisfies the system of equations as well as constraints. In the approach, an unknown state function $\eta(\aleph)$ and the control input $u(\aleph)$ are parameterized via neural networks. Specifically, the gain state function $\eta(\aleph)$ and the control input $u(\aleph)$ are neural networks. Specifically,

$$\eta(\aleph) \approx NN_h(\aleph, \theta), \quad u(\aleph) \approx NN_u(\aleph, \xi),$$

where NN_h and NN_u denote neural network models that have trainable parameters θ and ξ, respectively. This parametrization permits the networks to learn and adjust the system behavior during training yet satisfy the physics of the model.

5.2. Loss function construction

The PINNs approach uses a loss function that includes all the governing equations of the system being analyzed so that it is possible to learn in principle from the data and from any underlying physical laws. This loss function ensures that all predictions made by the network are constrained through the governing integro-differential equations and by appropriately chosen initial or boundary conditions. The total loss function is formulated as:

$$\text{Loss} = L_{\text{residual}} + L_{\text{initial}},$$

where the term L_{residual} is the residual error between the predicted output and the expected solution obtained from the governing equations. This residual loss is computed at various sampled points in the domain, thus ensuring that the predictions of the neural network satisfy the dynamics defined by the integro-differential equations. In other words, L_{residual} forces the neural network to minimize the mismatches between its predicted state and the real behavior of the system, according to the physical laws governing heat transfer. The term L_{initial} insists on the implementation of the initial condition of the system, that is, often given at the beginning of the time scale. This implies that the trained neural network complies with such an initial condition, thus its solution would appropriately begin in respect to the defined state of the system at some time $\aleph_0$. By including this initial condition in the loss function,

$L_{initial}$ makes sure that the model does not only fit the data but also has the correct configuration at the beginning, and this results in a better prediction at the end. Together, these two parts of the loss function, $L_{residual}$ and $L_{initial}$, steer the PINNs toward learning solutions that not only satisfy the physics of the underlying system but also the given initial conditions. This way, the model will be more reliable and robust in real-world applications.

5.3. Training process

The training process is focused on optimizing the parameters of the neural networks $NN_h(\aleph, \theta)$ and $NN_u(\aleph, \xi)$, which are designed to approximate the state function $\eta(\aleph)$ and control input $u(\aleph)$, respectively. The goal of this training is that these neural networks should represent the system's dynamics accurately and meet the constraints that are imposed by the fractional VFIDEs. These two goals have two major purposes: the primary goal is to follow the dynamics of the system, and that is accomplished by reducing the residual loss $L_{residual}$, thus ensuring that the outputs of these neural networks obey the governing equations, and the second one is to satisfy the given initial conditions of the problem, which is accomplished by adding the term $L_{initial}$, with any violation in those initial constraints. These are loss function components and guide the optimisation process that is usually undertaken with gradient-based methods, Adam or stochastic gradient descent (SGD), as used in repeatedly adjusting the parameters θ and ξ. The process of training should continue until it stabilizes into a minimal value within the loss function, meaning the neural networks correctly approximate the states and control inputs within the dynamical context of the system.

5.4. Dataset description

The training and validation dataset is constructed so as to simulate the dynamics of the heat transfer system. It comprises several key components: time points $\aleph$, which represent specific intervals where the state $\eta(\aleph)$ and control input $u(\aleph)$ are measured or predicted; measured state $\eta(\aleph)$, which comprises temperature readings at the corresponding time points; control input $u(\aleph)$, which indicates the applied heat source adjustments in watts at those time points; and the residual $\|cD^{\rho}\eta(\aleph) - RHS\|$, which represents the error between the neural network's predicted state and the expected value derived from the integro-differential equations. The dataset reflects all possible scenarios; it has variability in initial conditions and control strategies, which assures the robustness and generalization of the neural networks trained on it. For example, at time $\aleph_0 = 0$, the temperature of the initial state is 25°C. With an input heat source of 500 W, the smallest residual error of 0.002 is recorded. Similar occurrences are observed for later time intervals and are compiled in Table 1. These data sets become critical in terms of the good training and cross-validation of the proposed neural network models.

Time $\aleph$ (seconds)	Measured State $\eta(\aleph)$ (°C)	Control Input $u(\aleph)$ (W)	Residual $\|cD^{\rho}\eta(\aleph) - RHS\|$
$\aleph_0 = 0$	$\eta_0 = 25$	$u(\aleph_0) = 500$	0.002
$\aleph = 10$	30.5	480	0.003
$\aleph = 20$	35.2	450	0.005
$\aleph = 30$	40.0	420	0.001

Table 1: Example dataset for training and validation reflecting the dynamics of the heat transfer system.

5.5. Results and insights

The trained neural networks exhibit outstanding performance in the approximation of the state of the system and optimal control strategies. The state function $\eta(\aleph)$, represented by $NN_h(\aleph, \theta)$, accurately traces the temperature distribution as a function of time. Similarly, the control input $u(\aleph)$, represented by $NN_u(\aleph, \xi)$, gives a very accurate adjustment strategy to obtain the target state η^*. Another prominent

observation is that the small residual errors persist through the entire training domain. Therefore, solutions rendered by the neural network fulfill integro-differential equations appropriately. The capability to generalize into previously unseen conditions points to potential generalization through change in dynamics and, possibly delay or nonlinearity of a system. For instance, the model successfully transfers the system from an initial state $\eta(\aleph_0) = 25°C$ to a target state while optimizing the applied control effort. The performance metrics validate the network's reliability and accuracy, demonstrating its practical utility for real-world applications. We provide here the results obtained from all the different simulations and analyses, along with their graphical representation. These figures give different performances of the model as well as some insights regarding the state function, control input, prediction accuracy, and error analysis.

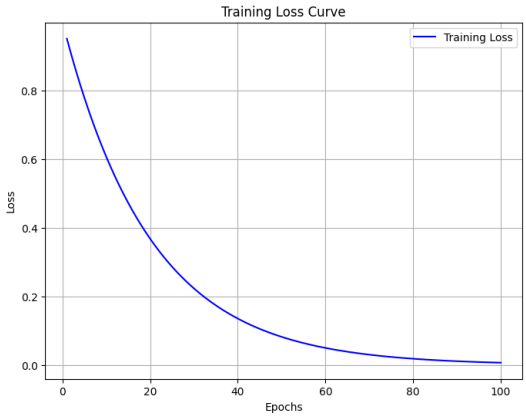

Figure 2: Training loss curve.

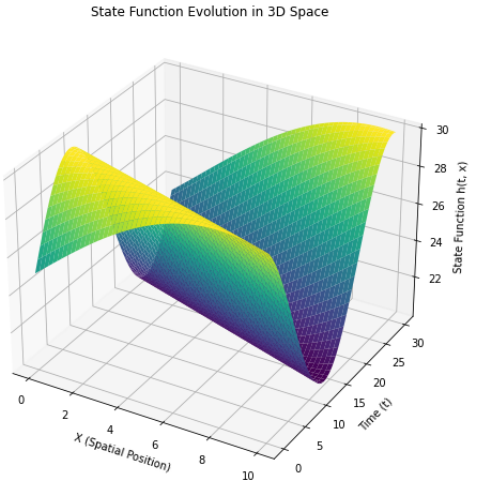

Figure 3: State function evolution in 3D space.

Plot 2 shows the training loss curve of the model in the training process. The exponential decay of the training loss over epochs indicates that the model is actually minimizing the loss function with time, achieving better performance as the training progresses. The curve demonstrates the convergence of the model and the effectiveness of the optimization process.

Figure 3 is a 3D surface plot representing the time and space evolution of the state function. The oscillation in the state function can be described as being forced by the sine term for its inherent dynamics. The surface of the above given representation describes how the state function varies with the spatial position and time.

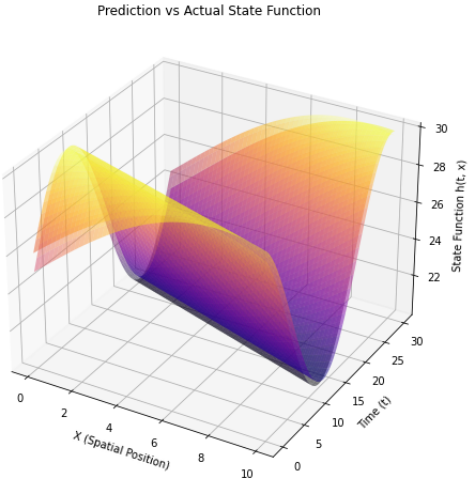

Figure 4: Prediction vs actual state function.

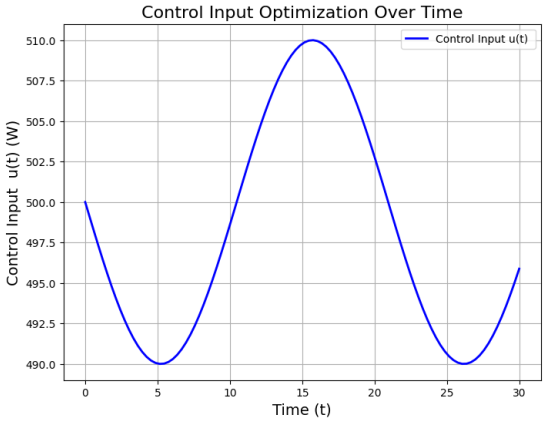

Figure 5: Control input optimization over time.

In this plot 4, we compare the predicted state function with the actual state function. The predicted

state is slightly shifted from the actual state, and this is an expected phenomenon given the inherent approximations of a model. Such a comparison clearly shows that this model can be used to predict the state of the system. However, minor deviations are observed; see the difference between the surfaces predicted and the actual surfaces in the figure below.

Figure 5 depicts the optimized control input in time that brings the system to the desired behavior. The periodic oscillation of the control input can be viewed as a means to bring the required change for system stability. Thus, optimizing the control input is very crucial in bringing the right state evolution for the system.

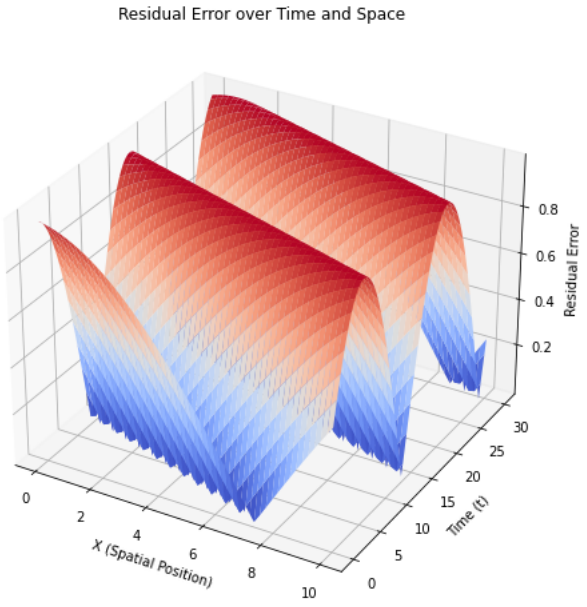

Figure 6: Residual error over time and space.

Plot 6 plots the residual error between the predicted and actual states over time and space. The error is growing as the model deviates from the actual state, thereby indicating regions in which the model prediction is not as accurate. Residual error is therefore essential for model performance understanding and for identifying regions in which discrepancies can be minimized. In summary, training loss curves indicate optimization is successful and the time evolution of the 3D state function and comparison between predicted and actual states depict the system's dynamics. Optimization of the input control ensures that the system's response will be what it is expected, and an error residue analysis provides details about places where more precision is needed from the model. Conclusive results are obtained through this procedure, with inherent knowledge on the behavior of the system and the efficiency of the current implementation.

5.6. Advantages of neural networks for controllability analysis

Neural networks, specially physics-informed neural networks, represent a state-of-the art method for dealing with fractional VIFDEs with SDD. In distinction from traditional approaches based on numeric methods, sometimes very expensive for large-scale implementations and difficult in practice, particularly for complex and complicated systems. The hybrid approach allows the PINNs to adapt to the nonlinearities and delays inherent in the system, without requiring explicit analytical solutions. The training is computationally efficient because it can converge quickly towards accurate solutions due to the employment of advanced optimization algorithms. Neural networks are highly flexible and have the ability to handle high-dimensional and dynamic systems, making it a versatile tool for diverse applications. The integration of PINNs ensures the solutions are accurate and robust in the face of variations in system parameters. Such solutions become of immense value to tackle complex problems of controllability and thus provide insights that are difficult to achieve using other conventional methods.

6. Conclusion

This paper explores the controllability of fractional VFIDEs with SDD. Using Caputo fractional derivatives and the semigroup properties of compact and analytic operators, under certain conditions we obtained controllability results in terms of Schauder's fixed point theorem. The above theoretical results have been justified by the detailed example provided, which explained the practical suitability of the result obtained. Numerical simulations have been carried out to prove the convergence of the solutions and present a sound illustration of the theory. Graphical analysis provided a deeper insight into the nature of the solutions by showing how the solutions behaved for different parameters. Besides analytical and numerical analyses, this paper presents the use of PINNs as a computational means for approximating the solutions and proving the controllability conditions. This integration of PINNs fills a gap between pure theoretical analysis and computational efficiency as it forms the basis of yet another new perspective to the numerous challenges facing these fractional systems characterized by SDDs. Further, combining such analytical, numerical, and ML-based approaches represents the versatility and pragmatic nature of this proposed method of approach to bring further innovation on the horizon about the analysis on the controllability of sophisticated fractional systems.

Acknowledgment

We would like to express my sincere gratitude to the reviewer(s) for their valuable time, constructive feedback, and insightful comments, which greatly contributed to improving the quality and clarity of this work.

Data availability

No data were used to support this study.

References

[1] R. P. Agarwal, B. D. Andrade, G. Siracusa, *On fractional integro-differential equations with state-dependent delay*, Comput. Math. Appl., **62** (2011), 1143–1149. 1
[2] P. Balasubramaniam, P. Tamilalagan, *Approximate controllability of a class of fractional neutral stochastic integro-differential inclusions with infinite delay by using Mainardi's function*, Appl. Math. Comput., **256** (2015), 232–246. 1
[3] M. Benchohra, F. Berhoun, *Impulsive fractional differential equations with state-dependent delay*, Commun. Appl. Anal., **14** (2010), 213–224. 1
[4] A. Columbu, S. Frassu, G. Viglialoro, *Refined criteria toward boundedness in an attraction-repulsion chemotaxis system with nonlinear productions*, Appl. Anal., **103** (2024), 415–431. 1
[5] A. Columbu, R. D. Fuentes, S. Frassu, *Uniform-in-time boundedness in a class of local and nonlocal nonlinear attraction-repulsion chemotaxis models with logistics*, Nonlinear Anal. Real World Appl., **79** (2024), 14 pages. 1
[6] Z. Dahmani, A. Taeb, *New existence and uniqueness results for high dimensional fractional differential systems*, Facta Univ. Ser. Math. Inform., **30** (2015), 281–293. 1
[7] A. Ganesh, S. Deepa, D. Baleanu, S. S. Santra, O. Moaaz, V. Govindan, R. Ali, *Hyers-Ulam-Mittag-Leffler stability of fractional differential equations with two Caputo derivative using fractional Fourier transform*, AIMS Math., **7** (2022), 1791—1810 1
[8] T. Guendouzi, L. Bousmaha, *Approximate controllability of fractional neutral stochastic functional integro-differential inclusions with infinite delay*, Qual. Theory Dyn. Syst., **13** (2014), 89–119. 1, 2
[9] T. Gunasekar, P. Raghavendran, S. S. Santra, D. Majumder, D. Baleanu, H. Balasundaram, *Application of Laplace transform to solve fractional integro-differential equations*, J. Math. Comput. Sci., **33** (2024), 225–237. 1
[10] T. Gunasekar, P. Raghavendran, S. S. Santra, M. Sajid, *Existence and controllability results for neutral fractional Volterra-Fredholm integro-differential equations*, J. Math. Comput. Sci., **34** (2024), 361–380. 1, 2.4
[11] T. Gunasekar, P. Raghavendran, S. S. Santra, M. Sajid, *Analyzing existence, uniqueness, and stability of neutral fractional Volterra-Fredholm integro-differential equations*, J. Math. Comput. Sci., **33** (2024), 390–407. 1, 2, 2.1, 2.2, 2.3, 2.5
[12] H. HamaRashid, H. M. Srivastava, M. Hama, P. O. Mohammed, E. Al-Sarairah, M. Y. Almusawa, *New numerical results on existence of Volterra–Fredholm integral equation of nonlinear boundary integro-differential type*, Symmetry, **15** (2023) 20 pages. 1

[13] A. Hamoud, *Existence and uniqueness of solutions for fractional neutral Volterra-Fredholm integro-differential equations*, Adv. Theory Nonlinear Anal. Appl., **4** (2020), 321–331. 1
[14] A. A. Hamoud, K. P. Ghadle, *Some new uniqueness results of solutions for fractional Volterra-Fredholm integro-differential equations*, Iran. J. Math. Sci. Inform., **17** (2022), 135–144. 1
[15] A. Hamoud, N. Mohammed, K. Ghadle, *Existence and uniqueness results for Volterra-Fredholm integro-differential equations*, Adv. Theory Nonlinear Anal. Appl.,**4** (2020), 361–372. 1
[16] E. Hernández, A. Prokopczyk, L. Ladeira, *A note on partial functional differential equations with state-dependent delay*, Nonlinear Anal. Real World Appl., **7** (2006), 510–519. 1, 2, 2.1, 2.2, 2.3
[17] Z. Jiao, I. Jadlovská, T. Li, *Global existence in a fully parabolic attraction-repulsion chemotaxis system with singular sensitivities and proliferation*, J. Differ. Equ., **411** (2024), 227–267. 1
[18] P. Kalamani, D. Baleanu, S. Selvarasu, M. Mallika Arjunan, *On existence results for impulsive fractional neutral stochastic integro-differential equations with nonlocal and state-dependent delay conditions*, Adv. Differ. Equ., **2016** (2016), 1–36. 1
[19] A. A. Kilbas, H. M. Srivastava, J. J. Trujillo, *Theory and applications of fractional differential equations*, Elsevier Science B.V., Amsterdam, (2006). 1
[20] T. Li, D. Acosta-Soba, A. Columbu, G. Viglialoro, *Dissipative gradient nonlinearities prevent δ-formations in local and nonlocal attraction-repulsion chemotaxis models*, Stud. Appl. Math., **154** (2025), 19 pages. 1
[21] T. Li, S. Frassu, G. Viglialoro, *Combining effects ensuring boundedness in an attraction-repulsion chemotaxis model with production and consumption*, Z. Angew. Math. Phys., **74** (2023), 21 pages. 1
[22] Z. Liu, M. Bin, *Approximate controllability for impulsive Riemann-Liouville fractional differential inclusions*, Abstr. Appl. Anal., **2013** (2013), 17 pages. 1
[23] F. Mainardi, P. Paradisi, R. Gorenflo, *Probability distributions generated by fractional diffusion equations*, arXiv preprint arXiv:0704.0320, (2007), 46 pages. 1
[24] A. Ndiaye, F. Mansal, *Existence and Uniqueness Results of VFIDEs via Caputo Fractional Derivative*, J. Math., **2021** (2021), 8 pages. 1
[25] I. Podlubny, *Fractional Differential Equations*, Academic Press, New York, (1999). 1
[26] P. Raghavendran, T. Gunasekar, J. Ahmad, W. Emam, *A Study on the Existence, Uniqueness, and Stability of Fractional Neutral Volterra-Fredholm integro-differential equations with State-Dependent Delay*, Fractal Fract., **9** (2025), 23 pages. 1, 3.2
[27] P. Raghavendran, T. Gunasekar, I. Ayoob, N. Mlaiki, *AI-driven controllability analysis of fractional impulsive neutral Volterra-Fredholm integro-differential equations with state-dependent delay*, AIMS Math., **10** (2025), 9342–9368. 1
[28] S. S. Santra *Oscillation criteria for nonlinear neutral differential equations first order with several delays*, Mathematica, **57(80)** (2015), 75–89. 1
[29] Y. Zhou, *Basic theory of fractional differential equations*, World Scientific Publishing Co. Pte. Ltd., Hackensack, NJ, (2014). 1, 2